Dynamics of manganese transport in the rat optic nerve evaluated using manganese-enhanced MRI (MEMRI)

Ø. Olsen[1], P. Goa[2], A. Kristoffersen[3], A. Sandvig[4], C. Brekken[2], and M. Thuen[2]

[1]Department of Radiography, Sør-Trøndelag University College, Trondheim, Norway, [2]Department of Circulation and Medical Imaging, Norwegian University of Science and Technology, Trondheim, Norway, [3]Department of Radiology, St Olavs Hospital, Trondheim, Norway, [4]Department of Laboratory Medicine Children's and Women's Health, Norwegian University of Science and Technology, Trondheim, Norway

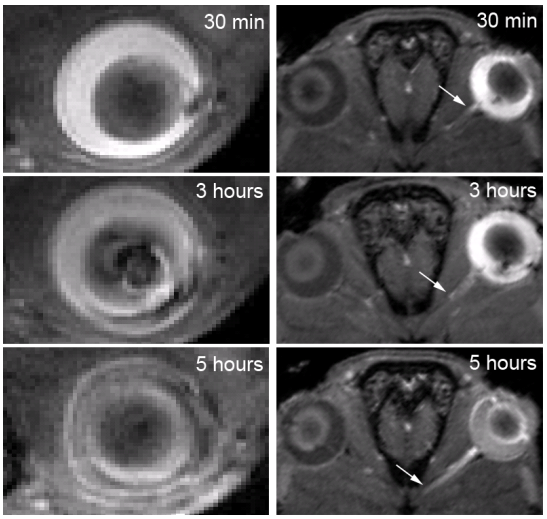

Figure 1: 2D slices from the vitreous body (left) and ON (right; reconstructed from continuous 2D slices perpendicular to the ON) at 30 min, 3 h and 5 h after injection of 3µl 50nM $MnCl_2$. The $MnCl_2$ is gradually cleared from the vitreous, while transported into the ON. The propagation of $MnCl_2$ is indicated by arrows.

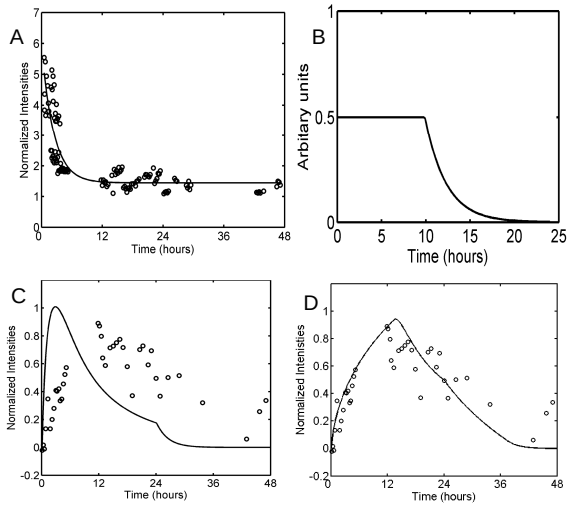

Figure 2: A: Mono-exponential fit to the vitreous body time-intensity curve. **B:** Input function where the concentration is constant until it reaches a specific level. This simulates a transport rate limited input of Mn^{2+} into the retinal ganglion cells. **C:** Simulated concentration curve (solid line) based on the mono-exponential fit to the vitreous body time-intensity curve (A) as input function. Dots are signal intensities measured 5 mm from the retina. Time of peak concentration appear earlier in the simulation than our observations. **D:** Simulated concentration curve (solid line) based on the constant concentration input function (B).

Introduction: Manganese-enhanced MRI (MEMRI) is an increasingly popular imaging method for animal MRI. However, little is known about the mechanisms and dynamics of manganese transport; which components inside the axons are involved in the transport, and what is the rate of the transport. Here, we investigate the dynamics of manganese transport by frequent, longitudinal MRI from the time of injection until 48 hours after injection.

Materials and Methods: Spraque Dowley rats (n=9) were given unilateral intravitreal injection of 3µl 50mM $MnCl_2$. In vivo MRI was obtained before and 0-6h, 12-30h and 42-44h and 46-48h after $MnCl_2$-injection. Each animal was in the scanner for 2h, and a 15-min T1-weighted MR-protocol was repeated. Isoflurane gas anaesthesia was used. For the time period 0-6h, 3-4 animals were used for each 2-hour time point (0-2h, 2-4h and 4-6h), while for all other time periods, one animal was used per 2-hour time point (12-14h, 14-16h, 16-18h etc.). Each animal was scanned 2-6 times. MRI was performed at 7T using a Bruker Biosped Avance 70/20 (Bruker Biospin, Ettlingen, Germany) with a 72 mm volume coil for transmission and an actively decoupled quadrature rat head surface coil for receive-only. Following the acquisition of scout images, a centric reordered saturation recovery turbo-FLASH sequence with saturation delay = 500 ms, flipangle=15 deg, TE/TR=2.7/9.25 ms and echo train length 445 ms was repeated every 15 min over the 2-hour period the animal was in the scanner. Starting in the vitreous body, 66 0.4mm slices perpendicular to the optic nerve (ON) was obtained with a matrix=192x192 and FOV=3.5x3.5cm^2. The data were normalized to the signal from a ROI placed in tissue in the same anatomical position in each animal and post processed using Matlab (R14 SP3, MathWorks Inc., Natick MA, USA). The co-ordinates of the ON centre were manually identified in each slice perpendicular to the nerve from the vitreous to the optic chiasm. The set of co-ordinates was re-sampled with 0.2 mm resolution by tri-linear interpolation which gave an intensity curve of the ON for each scan. The curves were integrated in 1mm steps to increase signal to noise ratio. In addition the intensity in the vitreous body was exctracted and normalized. A mono-exponential fit to the vitreous body time-intensity curve was performed and used as input function to the following model[1] for the transport of Mn^{2+} in the ON: $c(x,t) = M \exp[-(x-vt)^2 / 4D_x t - \lambda t] / A\sqrt{4\pi D_x t}$, where c is the concentration, x position, t time, v transport rate, λ clearance, D_x dispersion coefficient, M amount of injected tracer and A cross-sectional area of the ON. In addition we tested the model using an uptake-limited input-function (figure 2B) with constant effective concentration during 12 hours after injection. Transport rate, clearance and dispersion coefficients were manually adjusted to find a best fit between the model and the time-intensity curve in ON at 5 mm away from the eye.

Results and Discussion: The mono-exponential fit to the vitreous body time-intensity curve gave a clearance rate of 0.42 1/hours, which means that after 11.6 hours 99% of Mn^{2+} is cleared from the vitreous body. With this input function, it was not possible to fit the model to the measured time intensity curve, regardless of the choice of v, D and lambda. More precisely, the measured peak concentration is shifted to a later time-point than predicted from the transport model and the exponentially decaying input function. However, by using the constant concentration input function we were able to fit the model quite nicely with the measured data, see figure 2D. Moreover, the time to peak is robust against changes in transport rate, dispersion and clearance, indicating that this parameter is controlled by the input function.

In conclusion, our study indicate that the influx of Mn^{2+} into the retinal ganglion cells (RGC) through voltage gated Ca^{2+} channels is limited by the uptake rate through these channels rather than the Mn^{2+} concentration in the vitreous body, and plays an important role in estimating tracer kinetic parameters in this animal model.

References:

[1] Cross DJ, Flexman JA, Anzai Y, Maravilla KR, Minoshima S. *Age-related decrease in axonal transport measured by MR imaging in vivo*. Neuroimage. 2008 Feb 1;39(3):915-26.